ChemComm

This article can be cited before page numbers have been issued, to do this please use: Y. Tan, X. Yang, B. Li and D. Yuan, *Chem. Commun.*, 2016, DOI: 10.1039/C6CC08191F.

Volume 52 | Number 1 | 4 January 2016 | Pages 1–216

ChemComm

Chemical Communications
www.rsc.org/chemcomm

ISSN 1359-7345

ROYAL SOCIETY OF CHEMISTRY

COMMUNICATION
Marilyn M. Olmstead, Alan L. Balch, Josep M. Poblet, Luis Echegoyen *et al.*
Reactivity differences of $Sc_3N@C_{2n}$ (2*n* = 68 and 80). Synthesis of the first methanofullerene derivatives of $Sc_3N@D_{5h}$-C_{80}

175 YEARS

ROYAL SOCIETY OF CHEMISTRY

rsc.li/chemcomm

View Article Online
DOI: 10.1039/C6CC08191F

A table of contents entry

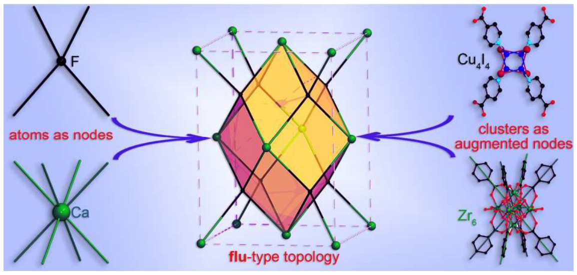

First heterometallic cluster-based Zr-MOF with *flu*-type topology was rationally designed by the cooperative assembly of $[Cu_4I_4(Ina)_4]^{4-}$ and $[Zr_6(\mu_3\text{-}OH)_8(OH)_8)]^{8+}$ clusters.

View Article Online
DOI: 10.1039/C6CC08191F

Journal Name

COMMUNICATION

Rational Design of *Flu*-Type Heterometallic Cluster-Based Zr-MOF

Yan-Xi Tan,[a] Xue Yang,[a,b] Bei-Bei Li,[a,b] and Daqiang Yuan*,[a]

Received 00th January 20xx,
Accepted 00th January 20xx

DOI: 10.1039/x0xx00000x

www.rsc.org/

Abstract Following the HSAB principle, the cooperative assembly of tetrahedral $[Cu_4I_4(Ina)_4]^{4-}$ metalloligands and 8-connecting $[Zr_6(\mu_3\text{-}OH)_8(OH)_8)]^{8+}$ building units leads to the first heterometallic cluster-based Zr-MOF (1). The results provide a successful strategy on rational design of heterometallic cluster-based Zr-MOF.

Zr(IV)-based metal-organic frameworks (Zr-MOFs) have been explored not only because of their designable structures,[1] high surface areas,[2] exceptional chemical stability,[3] but also because of the potential catalytic activity as heterogeneous catalysts.[4] Up to now, all of the reported Zr-MOFs are made up of monotonous zirconium clusters linked by multi-carboxylate ligands.[5] The cluster-based metalloligands remain rarely known in formation of heterometallic cluster-based Zr-MOFs,[6] because Zr(IV) as very hard acid has much stronger affinity to O atoms from carboxylic groups than those of other metallic ions. To address this problem, Hard-Soft-Acid-Base (HSAB) theory is a useful strategy toward heterometallic cluster-based Zr-MOFs to use organic ligands with different functional groups and different donor atoms, like O and N atoms. During the reaction process, the carboxylic acid can selectively coordinate to the in-situ formed Zr(IV) clusters and the N atoms can coordinate with other “soft” metal ions such as Cu(I) at the same time, thus inducing the formation of heterometallic Zr-MOFs. It is reported that the cooperative assembly of tetrahedral $[Cu_4I_4L_4]^{4-}$ metalloligands and metal-carboxylate clusters leads to some heterometallic 3d-3d MOFs.[7] Thus, the tetrahedral $[Cu_4I_4L_4]^{4-}$ metalloligand can reproduce the framework of the Zr-MOFs constructed by tetrahedral carboxylic ligands to form heterometallic cluster-based Zr-MOFs with two different inorganic building blocks. To date there are only a handful of Zr-MOFs that are composed of tetrahedral ligands,[8] in which just the two of them are fluorite (***flu***) topology (PCN-521 and MOF-841).[8a, 8e] The ***flu*** topology is especially intriguing for the construction of highly porous materials, because the structure can be conceived as large unoccupied dodecahedral cavities with Ca and F as vertexes.[9] Additionally, these frameworks with ***flu*** topology cannot undergo a translation in any direction without overlapping with themselves, leaving large dodecahedral cavities without self-interpenetration. To our knowledge, no experimental effort has focused on determining the heterometallic Zr-MOFs based on tetrahedral Cu_4I_4 cluster, which inspires us to explore the heterometallic cluster-based Zr-MOFs with ***flu*** topology. By employing symmetry-guided design, we propose to use the Zr-MOFs with ***flu*** topology as blueprint to construct heterometallic cluster-based Zr-MOFs (Scheme 1).

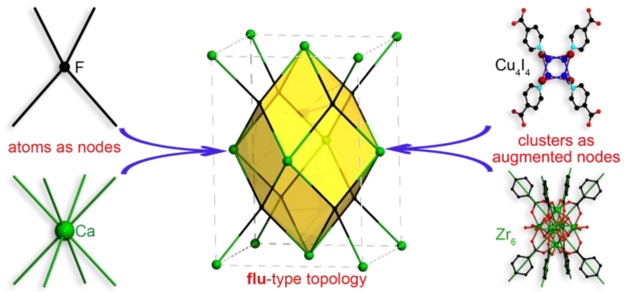

Scheme 1. Left and middle: A representation of the fluorite structure containing unoccupied dodecahedral cavities (yellow). Ca Green and F black. Right: The predictable fluorite structure results from rationally designed heterometallic cluster-based Zr-MOFs with two different clusters as augmented nodes. C black, O red, N sky blue and Zr green.

Here, we report the first heterometallic cluster-based Zr-MOF, namely $[Zr_6(\mu_3\text{-}OH)_8(OH)_8)][Cu_4I_4(Ina)_4]_2\cdot x$guest (**1**; Ina = isonicotinate). The three-dimensional (3D) ***flu***-type framework of **1** consists of 8-connecting $[Zr_6(\mu_3\text{-}OH)_8(OH)_8)]^{8+}$ building units linked by tetrahedral $[Cu_4I_4(Ina)_4]^{4-}$ metalloligands, and rich Zr-OH groups as Brønsted acid face the pores of dodecahedral cages. The Brønsted acid catalytic activity of **1** was evaluated by using the styrene oxide ring-opening

---

[a] State Key Laboratory of Structural Chemistry, Fujian Institute of Research on the Structure of Matter, Chinese Academy of Sciences, Fuzhou, 350002, Fujian, China. E-mail: ydq@fjirsm.ac.cn
[b] University of the Chinese Academy of Sciences, Beijing, 100049, China.

Electronic Supplementary Information (ESI) available: Experimental details, single-crystal structure determination, materials characterization (TGA, PXRD, NMR), GCMC simulation and typical experimental procedure for catalysis. CCDC 1507758. See DOI: 10.1039/x0xx00000x

View Article Online
DOI: 10.1039/C6CC08191F

reaction. The result shows that catalyst **1** has perfect catalytic activity and size selectivity during the test reaction of styrene oxide ring-opening reaction.

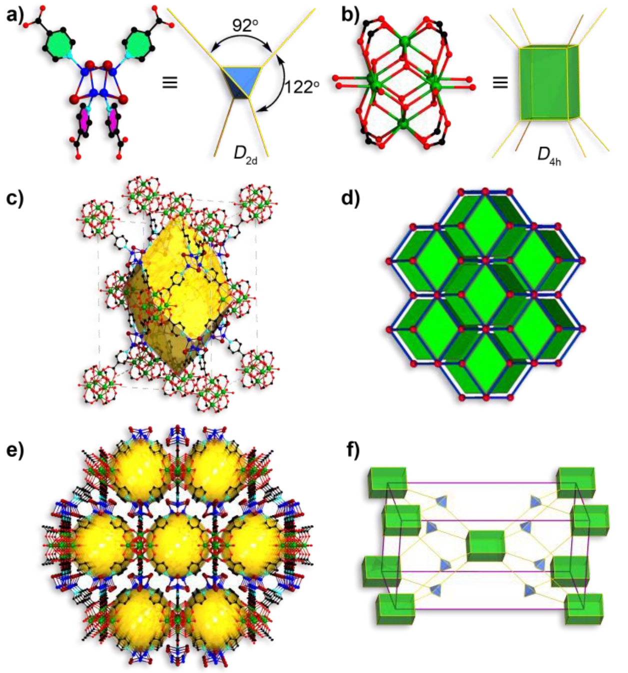

Fig. 1 a) The distorted conformation of the $[Cu_4I_4(Ina)_4]^{4-}$ metalloligand and its topological representation. (green and pink color highlight the benzoate rings lying in the mirror planes.) C black, O red, N sky blue, Cu blue, I crimson, Zr green. b) The 8-connected Zr_6 cluster and its topological representation. c) A dodecahedral cage with rhombic open faces, d) Natural tiling showing the packing of the dodecahedral cages (green tiles). e) View of the 3D porous framework of **1** along the a- or b-axis. The free spaces in the framework are presented as golden balls. f) The augmented ***flu*** topology of **1**, where the blue and cyan polyhedra represent 4- and 8-connected nodes, respectively.

Bright-yellow octahedral single crystals of **1**, formulated as $[Zr_6(\mu_3\text{-}OH)_8(OH)_8)][Cu_4I_4(Ina)_4]_2$, were obtained by a solvothermal reaction of zirconium *n*-propoxide, CuI, isonicotinic acid (HIna) and benzoic acid in a mixed solution of *N*,*N*-dimethylformamide (DMF) / ethanol (EtOH) at 100 °C for 12 h. Single-crystal X-ray diffraction reveals that compound **1** crystallizes in the tetragonal space group *I*4/mmm and consists of the 8-connected $[Zr_6(\mu_3\text{-}OH)_8(OH)_8]^{8+}$ clusters linked by tetrahedral $[Cu_4I_4(Ina)_4]^{4-}$ metalloligands (Fig. 1a). In each $[Zr_6(\mu_3\text{-}OH)_8(OH)_8]^{8+}$ cluster, all of the triangular faces are capped by μ_3-OH groups and eight edges are bridged by carboxylates from tetrahedral $[Cu_4I_4(Ina)_4]^{4-}$ metalloligands, while the remaining positions are occupied by terminal -OH groups. The $[Zr_6(\mu_3\text{-}OH)_8(OH)_8]^{8+}$ cluster in **1** has the same D_{4h} symmetry as reported ones in PCN-222, PCN-521 and PCN-523.[2c, 8a] Correspondingly, the symmetry of the tetrahedral $[Cu_4I_4(Ina)_4]^{4-}$ metalloligands is reduced from T_d to D_{2d} because the angles of two adjacent Ina ligands about 92° and 122°, which deviate ideal 109.47° in tetrahedron (Fig. 1a). This symmetry reduction makes the tetrahedral metalloligands symmetrically compatible with the $Zr_6(\mu_3\text{-}OH)_8(OH)_8]^{8+}$ clusters. In addition, four peripheral benzoates of the tetrahedral $[Cu_4I_4(Ina)_4]^{4-}$ metalloligands lie in two mirror planes. In the structure, each $[Zr_6(\mu_3\text{-}OH)_8(OH)_8]^{8+}$ SBU is surrounded by eight tetrahedral $[Cu_4I_4(Ina)_4]^{4-}$ metalloligands ligands, while each $[Cu_4I_4(Ina)_4]^{4-}$ links four $[Zr_6(\mu_3\text{-}OH)_8(OH)_8]^{8+}$ SBUs.

Moreover, in the whole framework, there is an open dodecahedral cage with a diameter of about 17.5 × 17.5 × 34.7 $Å^3$, which is formed by eight $[Cu_4I_4]$ tetrahedrons and six $[Zr_6(\mu_3\text{-}OH)_8(OH)_8]^{8+}$ SBUs as vertexes and twenty-four Ina ligands as edges (Fig. 1b). The face-centered cubic packing of these dodecahedral cages via sharing all of the rhombic facets further extend the structure into a 3D open framework (Fig. 1d and 1e). From the topological point of view, the $[Zr_6(\mu_3\text{-}OH)_8(OH)_8]^{8+}$ SBUs and tetrahedral $[Cu_4I_4(Ina)_4]^{4-}$ metalloligands can be regarded as 8- and 4-connecting nodes, respectively. Hence, the tetrahedral $[Cu_4I_4(Ina)_4]^{4-}$ metalloligands link to the $[Zr_6(\mu_3\text{-}OH)_8(OH)_8]^{8+}$ SBUs in a 2:1 ratio to form a 4,8-connected net with the ***flu*** topology (Fig. 1f), which has been known in two reported rigid Zr-MOFs (PCN-521 and MOF-841) based on the similar inorganic $[Zr_6(\mu_3\text{-}OH)_8(OH)_8]^{8+}$ units connected by organic ligands.[8a, 8d] It should be noted that **1** is the first MOF combined zirconium cluster and other metal cluster specie into its framework.

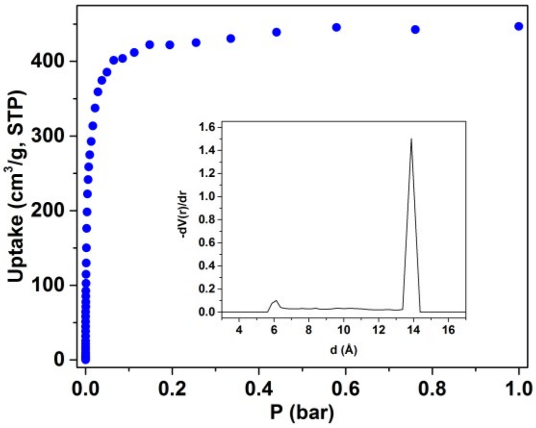

Fig. 2 The GCMC N_2 isotherms of **1** at 77.35 K. Insert: The simulated pore size distribution as seen by GCMC simulation for **1**.

Within these large dodecahedral cages, the framework of **1** possesses considerable void space, and the solvent accessible volume is estimated by PLATON to be about 69.7% of the total crystal volume. The dodecahedral cages are interconnected, thereby forming 3D open channels with an aperture diameter of 1.4 nm. On the basis of the crystal structure of **1**, high porosity and open channel, which are needed to efficiently transport substrate and product molecule to facilitate catalysis, are all obtained. However, N_2 adsorption measurements are unsuccessful to give the expected experimental Brunauer-Emmett-Teller (BET) specific surface area by adopting various activated methods such as traditional solvent exchange, freeze-drying and even supercritical CO_2 exchange (Fig. S3).[10] It might be attributed to framework distortion upon solvent removal, which is a common phenomenon observed for high porous MOFs.[11] Despite of that, powder X-ray diffraction patterns of fresh wet samples for **1**, as shown in Fig. S2, indicate that the frameworks are stable in some alcohols. It is very important for epoxide ring-opening reactions, which are

View Article Online
DOI: 10.1039/C6CC08191E

usually performed in alcohols solution. In order to better understand the pore structures, the atomistic Grand Canonical Monte Carlo (GCMC) simulations were performed to estimate the adsorption isotherms of N_2 at 77.35 K for **1** using RASPA2 code,[12] which implements the latest state-of-the-art algorithms for molecular dynamics. As show in the Fig. 2, the GCMC N_2 sorption of **1** clearly shows type-I isotherms. The calculated pore volume and the simulated BET surface areas for **1** are estimated as 0.67 cm^3/g and 1824 m^2/g, respectively. The inserted plot in Fig. 2 shows the simulated pore size distribution (PSD) by GCMC simulation for **1** without coordinated solvents. The PSD of **1** shows a peak at 13.6 Å, corresponding to the uniform dodecahedral cages in structure.

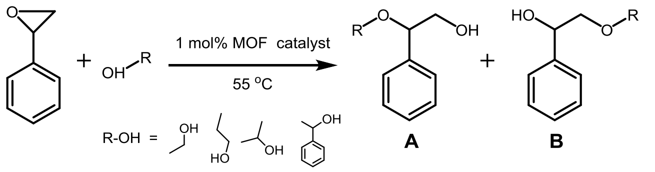

Scheme 2. Styrene oxide ring-opening reaction with mono alcohols, catalyzed by catalyst **1**.

As shown in Fig. 1c, Zr-OH groups face the dodecahedral cages in the MOF, which makes the catalytically active sites easily accessible. As the terminal hydroxides of defective Zr_6 nodes in **1** can function as Brønsted acid catalytic sites, we sought to test them as catalysts for the ring-opening of styrene oxide with a series of monohydric alcohols. In accordance with the two possible sites of nucleophilic attack of monohydric alcohols on styrene oxide, two products are possible: the primary alcohol (A, β-alkoxy alcohols) and the secondary alcohol (B). β-alkoxy alcohols as a kind of important synthetic intermediates can be used to synthesize alkoxy ketones or alkoxy acids, as well as some other special drug intermediate compounds.[13] As shown in Scheme 2, the reaction of styrene oxide and ethanol was carried out at 55 °C with 1 mol% MOF catalyst, with detailed procedures in the Electronic supplementary information (ESI). It is noted that no significant reactivity can be observed for this reaction in the absence of a catalyst because of the poor nucleophilicity of alcohols. The result affirmed that the *β*-alkoxy alcohol, *β*-ethoxy-2-phenylethanol, is the principal product confirmed by gas chromatography and ^{1}H NMR spectroscopy (Fig. S4-S7). After 8 hours, the reaction leaded to a 99.18% conversion of styrene oxide and a 95.31% selectivity of β-ethoxy-2-phenylethanol. After 24 hours, the final conversion of styrene oxide and selectivity of *β*-ethoxy-2-phenylethanol can be reached 100% and 95.21%, respectively. Judging from the powder X-ray diffraction (PXRD) patterns of the catalyst after ring-opening reaction, the framework of **1** is intact after usage as a catalyst (Fig. S2). Compared to the PXRD pattern of the as-synthesized sample, a slim redistribution of the peak intensities, but no change of the peak positions is observed. A recycling test with three consecutive runs was performed to check if catalyst **1** can be reused. For all three reactions, the conversion and regioselectivity after 24 hours are always in excess of 98% and 95%. The results indicate that catalyst **1** can be reused several times in this reaction without obvious reduced activity. To prove the heterogeneous mechanism of the reaction, leaching test of **1** was carried out by removing the solid catalyst after 1 h and continuing reaction for another 23 h. No further conversion was noted, proving heterogeneity of the catalyst.

Table 1. Highly efficient and selective styrene oxide ring-opening reactions catalyzed by catalyst **1**.

Entry	Alcohols	Time (h)	Conversion (%)	Selectivity (%)
1	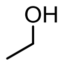	24[a]	trace	\[f]
3		0.5	26.52	95.12
4		1	49.61	95.15
5		2	79.13	95.02
6		4	94.70	95.02
7		8	98.81	95.31
8		12	99.06	95.19
9		24[b]	100.00	95.21
10		24[c]	99.5	95.16
11		24[d]	98.8	95.01
12		24[e]	49.62	95.18
13	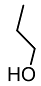	8	92.89	93.85
14		12	98.03	94.04
15		24	100.00	93.80
16	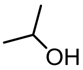	8	82.85	90.32
17		12	86.23	90.76
18		24	95.29	90.67
19	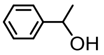	24	< 1	\[f]

[a] No catalyst **1**. [b] The first run. [c] The second run. [d] The third run. [e] The filtration test after reaction for 1 h. [f] Not calculated.

With these results in hand, we set out to change the substrates diverse in sizes to explore the relationship between catalytic activities and pore properties for catalyst **1**. Thus, ring-opening reactions of styrene oxide with other monohydric alcohols were performed to evaluate the catalytic activities of **1**, in which three kinds of monohydric alcohols with different sizes, shapes and nucleophilicity (Scheme 2 and Table 1) were employed. Still under the same conditions described above, the ring-opening reactions of styrene oxide with diverse monohydric alcohols were carried. It can be note that catalytic activities of **1** are dependent on the structural features of monohydric alcohols. As shown in Table 1, desired products are obtained but with different yields and regioselectivities. For two structural isomers *n*-propyl alcohol and isopropyl alcohol, although isopropyl group has stronger electron-donating ability than propyl group, isopropyl alcohol with large steric effect induces lower conversion and regioselectivity than *n*-propyl alcohol. For isopropyl alcohol, the catalytic activity is slightly lower than that of Zr-MOF-808 and Hf-MOF-808,[14] but much better than a series of UiO-type MOFs, such as Zr-UiO-66, Hf-UiO-66, Zr-UiO-67, Hf-UiO-67, Zr-PCN-57, Hf-PCN-57, Zr-NU-1000 and Hf-NU-1000.[14] Furthermore, no product can be obtained even after 24 h when the reaction was run with phenethyl alcohol as the nucleophile. This is consistent with our hypothesis that the narrow window size of the dodecahedral cages will hamper the diffusion of larger substrates and transfer of productions during catalytic reaction.

View Article Online
DOI: 10.1039/C6CC08191F

A tentative mechanism is proposed for the ring-opening reaction into β-alkoxy alcohols catalyzed by 1. First, the less-hindered O of epoxide is attacked by a proton from –OH to activate the epoxy ring, leaving a positively charged $O^{\delta+}$. Secondly, the electrons in β C–O bonds transfer to the $O^{\delta+}$, breaking the bond and effectively transferring the positive charge to the carbon. Thirdly, an oxygen atom from a nearby R-OH molecule attacks the electrophilic carbon from a direction opposite. The finally step is a rapid proton transfer to give the desired β-alkoxy alcohols and the catalytic species.

In summary, through the cooperative assembly of tetrahedral $[Cu_4I_4(Ina)_4]^{4-}$ metalloligands and Zr_6 clusters, the first heterometallic cluster-based Zr-MOF **1** has been successfully synthesized and structurally characterized as a high porous ***flu***-type network composed of the face-centered cubic packing of dodecahedral cages. Compound **1** with rich metal-bound Brønsted acid (M-OH) has notable catalytic activity on epoxide ring-opening reaction. The results reveal that catalytic activities of **1** are mainly dependent on the size and steric hindrance of alkyl substituent in primary alcohols. This work not only illustrates a successful case of designing heterometallic cluster-based Zr-MOFs with a desired topology, but also demonstrates that heterometallic cluster-based Zr-MOFs are potential catalysts for future applications.

This work was financially supported by the National Nature Science Foundation of China (21371169 and 21603229), the Strategic Priority Research Program of the Chinese Academy of Sciences (XDB20000000), and the Nature Science Foundation of Fujian Province (2016J01080).

References

1. (a) Y. Bai, Y. Dou, L. H. Xie, W. Rutledge, J. R. Li and H. C. Zhou, *Chem. Soc. Rev.*, 2016, **45**, 2327; (b) R. J. Marshall and R. S. Forgan, *Eur. J. Inorg. Chem.*, 2016, **2016**, 4310; (c) M. Kim and S. M. Cohen, *CrystEngComm*, 2012, **14**, 4096; (d) J. H. Cavka, S. Jakobsen, U. Olsbye, N. Guillou, C. Lamberti, S. Bordiga and K. P. Lillerud, *J. Am. Chem. Soc.*, 2008, **130**, 13850.
2. (a) T. C. Wang, W. Bury, D. A. Gomez-Gualdron, N. A. Vermeulen, J. E. Mondloch, P. Deria, K. Zhang, P. Z. Moghadam, A. A. Sarjeant, R. Q. Snurr, J. F. Stoddart, J. T. Hupp and O. K. Farha, *J. Am. Chem. Soc.*, 2015, **137**, 3585; (b) J. Zheng, M. Wu, F. Jiang, W. Su and M. Hong, *Chem. Sci.*, 2015, **6**, 3466; (c) D. Feng, Z. Y. Gu, J. R. Li, H. L. Jiang, Z. Wei and H. C. Zhou, *Angew. Chem. Int. Ed.*, 2012, **51**, 10307; (d) T. Liu, D. Feng, Y. Chen, L. Zou, M. Bosch, S. Yuan, Z. Wei, S. Fordham, K. Wang and H. Zhou, *J. Am. Chem. Soc.*, 2014, **137**, 413.
3. (a) G. Mouchaham, L. Cooper, N. Guillou, C. Martineau, E. Elkaim, S. Bourrelly, P. L. Llewellyn, C. Allain, G. Clavier, C. Serre and T. Devic, *Angew. Chem. Int. Ed.*, 2015, **54**, 13297; (b) D. A. Gomez-Gualdron, O. V. Gutov, V. Krungleviciute, B. Borah, J. E. Mondloch, J. T. Hupp, T. Yildirim, O. K. Farha and R. Q. Snurr, *Chem. Mater.*, 2014, **26**, 5632; (c) D. Feng, W. C. Chung, Z. Wei, Z. Y. Gu, H. L. Jiang, Y. P. Chen, D. J. Darensbourg and H. C. Zhou, *J. Am. Chem. Soc.*, 2013, **135**, 17105; (d) B. Wang, X. L. Lv, D. Feng, L. H. Xie, J. Zhang, M. Li, Y. Xie, J. R. Li and H. C. Zhou, *J. Am. Chem. Soc.*, 2016, **138**, 6204.
4. (a) D. Yang, S. O. Odoh, J. Borycz, T. C. Wang, O. K. Farha, J. T. Hupp, C. J. Cramer, L. Gagliardi and B. C. Gates, *ACS Catal.*, 2016, **6**, 235; (b) H. Fei and S. M. Cohen, *J. Am. Chem. Soc.*, 2015, **137**, 2191; (c) W. Y. Gao, H. Wu, K. Leng, Y. Sun and S. Ma, *Angew. Chem. Int. Ed.*, 2016, **55**, 5472; (d) Z. Li, N. M. Schweitzer, A. B. League, V. Bernales, A. W. Peters, A. B. Getsoian, T. C. Wang, J. T. Miller, A. Vjunov, J. L. Fulton, J. A. Lercher, C. J. Cramer, L. Gagliardi, J. T. Hupp and O. K. Farha, *J. Am. Chem. Soc.*, 2016, **138**, 1977; (e) K. Manna, P. Ji, F. X. Greene and W. Lin, *J. Am. Chem. Soc.*, 2016, **138**, 7488; (f) M. Rimoldi, A. Nakamura, N. A. Vermeulen, J. J. Henkelis, A. Blackburn, J. T. Hupp, J. F. Stoddart and O. K. Farha, *Chem. Sci.*, 2016, **7**, 4980; (g) X. Yu and S. M. Cohen, *J. Am. Chem. Soc.*, 2016, **138**, 12320.
5. (a) D. Alezi, I. Spanopoulos, C. Tsangarakis, A. Shkurenko, K. Adil, Y. Belmabkhout, O. K. M, M. Eddaoudi and P. N. Trikalitis, *J. Am. Chem. Soc.*, 2016, **138**, 12767; (b) C. X. Chen, Z. Wei, J. J. Jiang, Y. Z. Fan, S. P. Zheng, C. C. Cao, Y. H. Li, D. Fenske and C. Y. Su, *Angew. Chem. Int. Ed.*, 2016, **55**, 9932; (c) B. Li, B. Gui, G. Hu, D. Yuan and C. Wang, *Inorg. Chem.*, 2015, **54**, 5139.
6. (a) W.-X. Zhang, P.-Q. Liao, R.-B. Lin, Y.-S. Wei, M.-H. Zeng and X.-M. Chen, *Coord. Chem. Rev.*, 2015, **293-294**, 263; (b) L. Huang, S. S. Wang, J. W. Zhao, L. Cheng and G. Y. Yang, *J. Am. Chem. Soc.*, 2014, **136**, 7637.
7. (a) Y.-X. Tan, Y.-P. He and J. Zhang, *Chem. Mater.*, 2012, **24**, 4711; (b) J. Qian, F. Jiang, K. Su, J. Pan, Z. Xue, L. Liang, P. P. Bag and M. Hong, *Chem. Commun.*, 2014, **50**, 15224; (c) X. X. Li, Y. X. Wang, R. H. Wang, C. Y. Cui, C. B. Tian and G. Y. Yang, *Angew. Chem. Int. Ed.*, 2016, **55**, 6462; (d) H. He, F. Sun, S. Ma and G. Zhu, *Inorg. Chem.*, 2016, **55**, 9071.
8. (a) M. Zhang, Y. P. Chen, M. Bosch, T. Gentle, 3rd, K. Wang, D. Feng, Z. U. Wang and H. C. Zhou, *Angew. Chem. Int. Ed.*, 2014, **53**, 815; (b) P. Ji, K. Manna, Z. Lin, A. Urban, F. X. Greene, G. Lan and W. Lin, *J. Am. Chem. Soc.*, 2016, **138**, 12234; (c) X. Zhang, X. Zhang, J. A. Johnson, Y. S. Chen and J. Zhang, *J. Am. Chem. Soc.*, 2016, **138**, 8380; (d) H. Furukawa, F. Gandara, Y. B. Zhang, J. Jiang, W. L. Queen, M. R. Hudson and O. M. Yaghi, *J. Am. Chem. Soc.*, 2014, **136**, 4369; (e) S. Wang, J. Wang, W. Cheng, X. Yang, Z. Zhang, Y. Xu, H. Liu, Y. Wu and M. Fang, *Dalton Trans.*, 2015, **44**, 8049.
9. (a) H. Chun, D. Kim, D. N. Dybtsev and K. Kim, *Angew. Chem. Int. Ed.*, 2004, **43**, 971; (b) M. Dinca, A. Dailly and J. R. Long, *Chem. Eur. J.*, 2008, **14**, 10280; (c) J. M. Gotthardt, K. F. White, B. F. Abrahams, C. Ritchie and C. Boskovic, *Cryst. Growth Des.*, 2012, **12**, 4425.
10. (a) M. R. Lohe, M. Rose and S. Kaskel, *Chem. Commun.*, 2009, 6056; (b) J. E. Mondloch, O. Karagiaridi, O. K. Farha and J. T. Hupp, *CrystEngComm*, 2013, **15**, 9258.
11. (a) F. Song, C. Wang, J. M. Falkowski, L. Ma and W. Lin, *J. Am. Chem. Soc.*, 2010, **132**, 15390; (b) C. Serre, F. Millange, C. Thouvenot, M. Noguès, G. Marsolier, D. Louër and G. Férey, *J. Am. Chem. Soc.*, 2002, **124**, 13519; (c) P. L. Llewellyn, G. Maurin, T. Devic, S. Loera-Serna, N. Rosenbach, C. Serre, S. Bourrelly, P. Horcajada, Y. Filinchuk and G. Ferey, *J. Am. Chem. Soc.*, 2008, **130**, 12808; (d) Z. Ju, S. Yan and D. Yuan, *Chem. Mater.*, 2016, **28**, 2000.
12. D. Dubbeldam, S. Calero, D. E. Ellis and R. Q. Snurr, *Mol. Simulat.*, 2015, **42**, 81.
13. (a) S. M. Bruno, A. C. Gomes, T. S. Oliveira, M. M. Antunes, A. D. Lopes, A. A. Valente, I. S. Goncalves and M. Pillinger, *Org. Biomol. Chem.*, 2016, **14**, 3873; (b) X. Gao, X. Pan, J. Gao, H. Jiang, G. Yuan and Y. Li, *Org. Lett.*, 2015, **17**, 1038; (c) R. F. Mendes, M. M. Antunes, P. Silva, P. Barbosa, F. Figueiredo, A. Linden, J. Rocha, A. A. Valente and F. A. Almeida Paz, *Chemistry*, 2016, **22**, 13136.
14. Y. Liu, R. C. Klet, J. T. Hupp and O. Farha, *Chem. Commun.*, 2016, **52**, 7806.